CAO, W., WANG, S.-L., FERNANDEZ, C., ZOU, C.-Y., YU, C.-M. and LI, X.-X. 2019. A novel adaptive state of charge estimation method of full life cycling lithium-ion batteries based on the multiple parameter optimization. *Energy science and engineering* [online], Early View. Available from: https://doi.org/10.1002/ese3.362

A novel adaptive state of charge estimation method of full life cycling lithium-ion batteries based on the multiple parameter optimization.

CAO, W., WANG, S.-L., FERNANDEZ, C., ZOU, C.-Y., YU, C.-M. and LI, X.-X.

2019

Received: 15 April 2019 | Revised: 30 April 2019 | Accepted: 3 May 2019

DOI: 10.1002/ese3.362

RESEARCH ARTICLE

Energy Science & Engineering Open Access

A novel adaptive state of charge estimation method of full life cycling lithium-ion batteries based on the multiple parameter optimization

Wen Cao[1] | **Shun-Li Wang**[1] | **Carlos Fernandez**[2] | **Chuan-Yun Zou**[1] | **Chun-Mei Yu**[1] | **Xiao-Xia Li**[1]

[1]School of Information Engineering, Southwest University of Science and Technology, Mianyang, China

[2]School of Pharmacy and Life Sciences, Robert Gordon University, Aberdeen, UK

Correspondence
Shun-Li Wang, School of Information Engineering, Southwest University of Science and Technology, Mianyang 621010, China.
Email: 497420789@qq.com

Funding information
National Natural Science Foundation of China, Grant/Award Number: 61801407

Abstract

The state of charge (SoC) estimation is the safety management basis of the packing lithium-ion batteries (LIB), and there is no effective solution yet. An improved splice equivalent modeling method is proposed to describe its working characteristics by using the state-space description, in which the optimization strategy of the circuit structure is studied by using the aspects of equivalent mode, analog calculation, and component distribution adjustment, revealing the mathematical expression mechanism of different structural characteristics. A novel particle adaptive unscented Kalman filtering algorithm is introduced for the iterative calculation to explore the working state characterization mechanism of the packing LIB, in which the incorporate multiple information is considered and applied. The adaptive regulation is obtained by exploring the feature extraction and optimal representation, according to which the accurate SoC estimation model is constructed. The state of balance evaluation theory is explored, and the multiparameter correction strategy is carried out along with the experimental working characteristic analysis under complex conditions, according to which the optimization method is obtained for the SoC estimation model structure. When the remaining energy varies from 10% to 100%, the tracking voltage error is <0.035 V and the SoC estimation accuracy is 98.56%. The adaptive working state estimation is realized accurately, which lays a key breakthrough foundation for the safety management of the LIB packs.

KEYWORDS

full life cycle, lithium-ion batteries, multiple parameter optimization, particle adaptive unscented Kalman filter, splice equivalent model, state of charge estimation

1 | INTRODUCTION

As the scale of energy development and utilization continues to expand, the energy and environmental issues become the hot topics of common concern gradually in the world. The promotion and application of the new energy construction have reached consensus on a global scale, which is also the energy revolution and restructuring strategy.[1] The lithium-ion

batteries (LIB) have the advantages of high energy density, long life, and high output power performance. The packing application plays an important role in optimizing energy structure, ensuring energy supplies, and promoting decontamination reduction, which is an important part of the new energy field.[2] The power applications such as large-scale energy storage, new electric vehicle (EV), and drones must be safe and cost-effective in the whole life cycle.[3] Under the mega trend of the new energy boom, the LIBs are growing at a rate of more than 50% per year. However, its safety problem becomes prominent increasingly and more than 40 EV fires occurred in just 2018, 70% of which were caused by packing safety management problems.[4]

The power LIB pack is constructed by the multicell cascading to realize the high-power application and provide the required energy. It has the characteristics of large capacity, large number of series-parallel sections, and strict safety boundary requirements. Therefore, the associated battery management system (BMS) is required, in which the real-time condition monitoring and security control should be performed to ensure its safety, power, and durability. Among them, the effective equivalent modeling and accurate state of charge (SoC) estimation are key technologies in the BMS.[3] The LIB pack belongs to a complex electrochemical system, which is different from general industrial control objects. The accuracy of SoC estimation is difficult to be improved, which affects the effectiveness of BMS seriously and even attracts the safety accident.[5] The development of the power LIB application and safety management has entered an important period of difficult problems.[6]

The equivalent modeling is the basis of obtaining the battery characteristics and mathematical expression in the working state estimation process.[7] Therefore, the accurate SoC estimation plays an important role in improving the overall performance, which is of great significance for the remaining power forecasting and safety guarantee.[8] Due to the influence of the internal structure and environmental conditions, there are many noises in the external measurement parameters.[9] It is very difficult to extract and express the feature information mathematically.[10] Therefore, the packing equivalent modeling and state estimation method are the key to suppress the safety threat to the LIB packs, and it is of great significance to improve its energy conversion efficiency and extending its service life.

The equivalent modeling is one of the key directions of international new energy research,[11] and the research institutes have also carried out research simultaneously and achieved fruitful results,[12] which provide an important reference to the SoC estimation. The LIB operation involves multiple electrochemical coupling reaction processes and therefore has strong nonlinear dynamic characteristics.[13] The equivalent modeling is the basis of subsequent state estimation and safety management, which can realize the mathematical description of the state-space equation and has a wide range attention.[14,15]

In order to describe the dynamic characteristics of LIBs, the equivalent modeling [16] mainly includes the electrochemical model and the equivalent circuit model (ECM) types.[17] The electrochemical model builds empirical mathematical equations by analyzing the internal physical mechanism and electrochemical reaction of the battery. And the simplified application is applied to reduce the computational complexity and improve the simulation accuracy on this basis.[18,19] The ECM belongs to the semimechanism semiempirical model, in which the mathematical circuit expression is used to simulate the battery behavior by using the circuit elements such as voltage source, resistor, capacitor, and inductors.[20] The key and foundation of this type of model is the circuit and electronic components.[21,22] The electrical modeling method is used to simulate the working process regardless of its internal chemical reaction and therefore has good applicability.[23]

The LIBs often exhibit some resistance-capacitance (RC) characteristics during the charge-discharge process [24] and further consider the hysteresis of open-circuit voltage (OCV) after the charge-discharge time period.[25] The problem with this equivalent modeling method is that a simple model cannot reflect the dynamic changes of the battery and may lead to incorrect recognition results.[26] However, there are too many parameters to be determined in the complex model and the calculation amount will be increased greatly, which may bring about parameter divergence problems.[27] An enhanced ECM was constructed by Wei et al[28] for the charge redistribution and temperature effect studies. An nonlinear fractional-order estimator was built with guaranteed robustness and stability for the SoC indication of the LIBs.[29] A new parameter identification method was proposed by considering electrochemical properties.[30] An equivalent circuit of 10 parameters was designed, and an evaluation study of electrochemical characterization was carried out by Wang et al[31] A mathematical model was also constructed to express the thermal behavior of the LIB pack during overcharging process.[32] A practical model was also constructed for the energy and voltage response state prediction including temperature and aging effects.[33] The parameter estimation and sensitivity analysis were carried out by using the electrochemical models for the LIBs,[34] which was coupled with the thermal model and used to describe the thermal performance during the cycling charge-discharge process.[35] The degradation state prediction was explored in the whole climate,[36] and the identification was conducted for different ECM parameters along with the global optimization.[37]

As the complex series-parallel combination is used in the LIB packs to break for the limitations of cell voltage and capacity, there are differences in cell-to-cell consistency and interaction.[38] The phenomenon of spontaneous combustion of the LIB pack caused by the invalid safety management

poses a great threat to the energy security.[39] Therefore, the breakthrough of the ECM modeling is especially important to the energy management, which is also an effective means to avoid the safety accidents.[40] Under the influence of the complex cell combination structure, the ECM is the key to improve its energy utilization efficiency and safety.[41,42] The parameters such as ohmic internal resistance, polarization resistance, and capacitance in the ECM also need to be measured indirectly by the experimental means.[43] Therefore, the mathematical description can only be achieved by using the external measurable parameters such as voltage, current, and temperature.[44,45]

The SoC is an important parameter reflecting its remaining available power. The current integration, OCV, Kalman Filter (c) and its expansion algorithm, particle filtering (PF), and neural network (NN) have been explored gradually and applied to the SoC estimation of the LIBs.[46] The load-responsive model switching SoC estimation was investigated on the LIBs, and an event trigger procedure was developed to detect the estimation performance by leveraging the high-pass filter and coulomb counting algorithms.[47] By analyzing the influence of the heat, voltage, and internal resistance of the heat dissipation mode, a thermal management strategy was proposed to adjust its temperature rise and uniformity.[48] An equivalent model was constructed by the physical property analysis that is easy to parameterize.[49] A comparative study was conducted on the comprehensive model identification.[50] A model-based SoC observer was constructed, and the error analysis was performed as well.[51] An adaptive SoC estimation was conducted by using the separation battery model,[52] which is also realized by the adaptive Extended Kalman filter (EKF) and wavelet transform matrix.[53] The multitimescale observer was designed for the SoC estimation of the LIBs, in which the design parameter sets could be tuned in different timescales.[54] The accurate power allocation strategy was studied for the SoC balancing treatment of the distributed DC microgrid,[55] which was also achieved by a dual EKF algorithm and the charging voltage curve.[56] Through the estimating result, it can be further estimated on how long the battery is going to last for even a dynamic power demand.[57]

The existing research has achieved remarkable results in the equivalent model construction and SoC estimation. The packing ECM modeling and SoC estimation of complex conditions still need to be further developed. Therefore, it is necessary to build the battery equivalent model that is adaptive to the complex operating conditions by the modular circuit characterization to improve its accuracy. The external measurable parameter characteristic information is used to establish the time-dependent equivalent model, which is described by using the state-space equations to realize the accurate working characteristic expression. Combined with the influencing factor analysis, the modified strategy is designed to eliminate the inconsistency impact on the packing SoC estimation. A new SoC estimation method is proposed by using the improved iterative calculation algorithm, which provides the theoretical guarantee of the LIB power application safety.

2 | MATHEMATICAL ANALYSIS

The change in key factors can be obtained by considering the battery cascading influence and aging process, according to which the accurate mathematical expression is realized by the ECM modeling and optimization. Furthermore, the Reduced Particle Adaptive Unscented Kalman Filter (RP-AUKF) algorithm is designed to realize the loop iterative SoC estimation. Based on the equivalent modeling and state estimation algorithm, the model parameter correction is investigated to eliminate the influence of the cell-to-cell difference, and the iterative calculation model with adaptive ability is constructed, which lays a theoretical foundation for the efficient management of the LIB packs.

2.1 | Equivalent modeling

The LIB pack power supply has high requirements for its safety. Because of its complex signal characteristics, a high-reliability filtering scheme is designed to achieve the accurate extraction of its effective information. Considering the influence of temperature gradient changes, the signal correction methods that are studied are suitable for different ambient temperatures. By investigating the mechanism analysis and working condition simulation experiments, the variation on the key factors can be obtained. Using the Hybrid Pulse Power Characteristic (HPPC) experimental test method, the model parameters are identified effectively, and their changing rules are obtained to describe their dynamic working characteristics. Considering the value change in each parameter along with the change in working conditions, the mathematical expression of the dynamic equivalent model can be realized. The balance state evaluation is realized by combining variance and coefficient of variation in the equivalent modeling process of the LIB pack, which is applied to eliminate the inconsistency influence over the internal battery cells.

According to the working state description purpose of the battery pack, the characteristic performance and computational complexity should be considered comprehensively, according to which the ECM modeling effect analysis is carried out. The modeling process is based on experimental data, and the equivalent circuit method is used to simulate its working process, which has strong applications. By assuming that all of the internal battery cells are identical, the entire battery pack is equivalent to be a battery cell having higher voltage and larger capacity, and the balance state is introduced to characterize the intercell inconsistency. Combining the

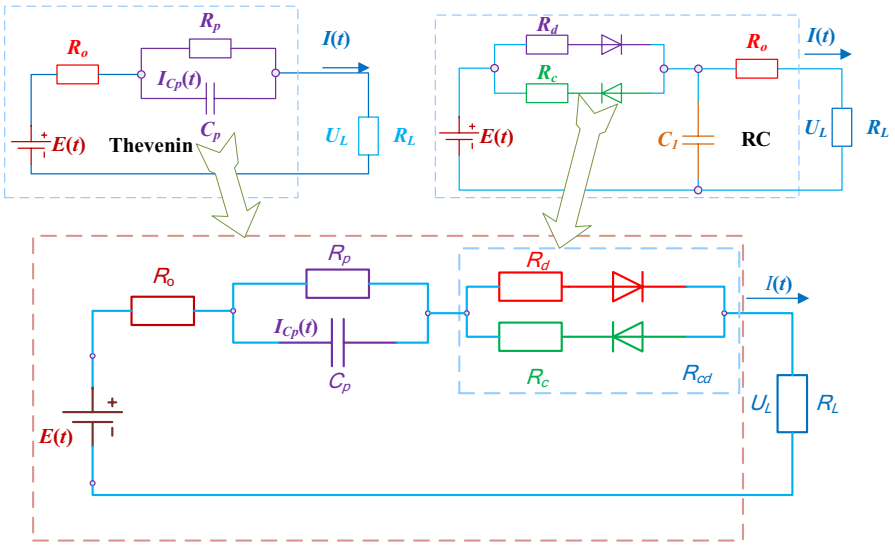

FIGURE 1 The improved equivalent model

advantages and disadvantages of various equivalent methods, the application and targeted improvement on various equivalent models are explored. The improved equivalent model construction can be obtained in order to describe the functional relationship between different model parameters in the iterative calculation process and realize the mathematical state-space expression.

The improved equivalent model uses the ideal voltage source U_{oc} to describe the OCV characteristics. The internal resistance R_o of the ohmic effect is connected serially, and the one-order RC parallel loop is used to characterize its polarization effect and improve the accuracy of the battery operation state. On the basis of the equivalent simulation, a parallel resistance circuit is used with a reverse diode connected with series, in combination with the resistance R_c and R_d to characterize the resistance difference during charging and discharging processes. By considering the influence of these factors comprehensively, an effective solution is proposed to provide the solution to packing LIB equivalence problem and its state-space equation description is realized. Combined with the application scenario and working characteristics analysis of the LIB pack, the ECM constructing process is shown in Figure 1.

By the improvement on the original Thevenin and RC equivalent models, the mathematical description of the working characteristics of the LIB pack is obtained. This is combined with the simulation analysis of the working conditions. The parameter description is described as follows. $E(t)$ indicates the OCV state. R_o characterizes the ohmic effect, which is used to describe the internal resistance when the LIB is in the stable state without charge and discharge. R_c and R_d are used to characterize the resistance difference when the LIB is in the dynamic SoC and discharge working process, which describes the voltage drop between the positive and negative electrodes of the LIB pack during charge-discharge time period. The parallel RC circuit is used to simulate the polarization effect. R_p is used to characterize the polarization resistance, and C_p is the polarization capacitance. R_d is the internal resistance difference in discharge, and R_c is the internal resistance difference in the charging process. $U_L(t)$ is the closed circuit voltage (CCV) between the positive and negative electrodes after the LIB pack is connected to the external circuit. $I_L(t)$ is a charge-discharge current.

2.2 | Mathematical *description*

According to the improved ECM, the mathematical description method of the circuit is used to realize the state-space representation of the equivalent model. The basic experimental analysis is combined with the multivariate nonlinear parameter estimation, and the model parameter identification method is developed to establish the state parameters and their weights. The model parameter verification and error suppression are completed, and the mathematical description method of the equivalent model is studied. The functional relationship of the iterative calculation is described for the mathematical expression of the state equation in the SoC estimation process. The SoC value of the prediction link is obtained by the ampere-hour (Ah) integration. The state equation in the continuous-time state-space description is shown in Equation (1).

$$S(t) = S(0) - \int_0^t \frac{\eta_I \eta_T I(\tau)}{Q_n} d\tau. \quad (1)$$

In the above expression, $S(t)$ represents the SoC value at the time point of t, and $S(0)$ is its initial value. η_I denotes the coulombic efficiency corresponding to the current I. η_T shows the temperature effect on the coulomb efficiency η. Q_n is the rated capacity.

Aiming to realize the accurate characterization under complex working conditions, the coefficient of the model

parameters can be obtained by conducting the experimental data analysis. Then, the observational representation can be obtained together with its state-space description, which lays the foundation for the state estimation model construction. According to Kirchhoff Voltage Law (KVL), the observation equation can be obtained as shown in Equation (2).

$$R_o I(t) + U_p + I(t) R_{cd} = E(t) - U_L(t). \quad (2)$$

The electromotive force $E(t)$ equals to the U_{oc} of the battery pack numerically. Meanwhile, the Ohm resistance is characterized by R_o. R_p is the polarization resistance and C_p the polarization capacitance. U_L is the CCV after the LIB pack is connected to an external circuit. R_d is the discharging internal resistance, and R_c is the charging resistance. In order to simplify the state-space equation description process, $R_{cd}(t)$ is used to characterize the differential resistances of R_c and R_d. According to the acquisition goal of observation equation, it can be transformed and combined with the model structure analysis. The transformation expression of the observation equation is shown in Equation (3).

$$U_L(t) = E(t) - R_o I(t) - U_p - I(t) R_{cd}. \quad (3)$$

In the equivalent model, τ is the time constant of the parallel RC circuit, which is calculated by $\tau = R_p C_p$. R_p is the polarization resistance. The RC iterative loop voltage calculation process is shown in Equation (4).

$$U_p(k) = I(k) R_p \left(1 - e^{-T_s / R_p C_p}\right). \quad (4)$$

In the above expression, $U_p(k)$ is the voltage across the polarization resistor. $I(k)$ is the current, and T_s is the sampling time interval constant. R_p is the polarization resistance, and C_p is the polarization capacitance. The $U_p(k)$ expression is substituted for the $U_L(t)$ calculation, which can be discretized to obtain the final observation equation as shown in Equation (5).

$$U_L(k) = E(t) - R_o I(k) - I(k) R_p \left(1 - e^{-T_s / R_p C_p}\right) - I(k) R_{cd}. \quad (5)$$

The mathematical description process does not need to introduce the complex mathematical models, which provides great feasibility for the rapid error analysis of the identification results. The observation equation describes the CCV signal state for the LIB pack. As can be known from the OCV-based calculation process, the identification results are closely related to the CCV value. In order to achieve the goal of accurate parameter identification, the output voltage of the LIB pack is set as the output parameter. Combined with the influence of the working current and temperature, the model parameters are analyzed and identified with the LIB pack. Weighing the accuracy and complexity of the model parameter identification, the state-space equation description method is optimized. When the LIB pack is in the charge-discharge state, the direction of the discharging current is specified as positive, according to which the state and observation equations are combined together to construct the packing equivalent model. The modeling state-space description is shown in Equation (6).

$$\begin{cases} S(k|k-1) = S(k-1) - \dfrac{\eta_I \eta_T I(k) T_s}{Q_n}{}_s + w(k) \\ U_L(k) = E(t) - R_o I(k) - I(k) R_p \left(1 - e^{-T_s / (R_p C_p)}\right) - I(k) R_{cd} + v(k), \end{cases} \quad (6)$$

wherein, k is the time point at which the LIB pack is modeled equivalently. The state-space variable S is the SoC value of the LIB pack, and $U_L(k)$ is the CCV value. R_o is the ohmic internal resistance of the LIB pack, and $I(k)$ is the output current. T_s is the detection period of the battery pack parameters, that is, the signal sampling time interval. $U_p(k)$ is the voltage value of the polarization resistor. The control variable $I(k)$ is the current. R_p is the polarization resistance, and C_p is the polarization capacitance. E is the ideal voltage source equivalent parameter that characterizes the OCV value of the battery pack. At the same time, the parallel circuit of R_p and C_p is used to reflect the generation and elimination of the polarization influence. The observed variable U_L is the CCV value after the LIB pack is connected to the external circuit, which is obtained by conducting the real-time measurement of the working process. The system noise is $w(k)$, and its covariance is Q. The observed noise is $v(k)$, and its covariance is R.

2.3 | Collaborative estimation

Because of its recessive state quantities, the SoC estimation is transformed into the implicit state estimation problem of the nonlinear time-varying systems. In order to solve this problem, the battery performance is first tested to determine the main factors affecting its performance and changing law. Then, the battery model is established by using the mechanism, semiempirical or empirical modeling method. Finally, the model-based battery state observer is designed. Combined with the state-space expression of the LIB pack and the recursive iterate calculation of probability density function, the suitable SoC estimation method is studied for the high noise immunity, high robustness, and fast convergence. According to the constructed ECM and its state-space equation, the state equation is used to solve the nonlinear transfer function of mean and covariance by using the unscented transform (UT) technique. Furthermore, the theoretical research on the state estimation of nonlinear dynamic systems driven by non-Gaussian noise is carried out to realize the synchronization estimation.

According to the packing equivalent model and its state-space description, the modeling peculiarity is analyzed under

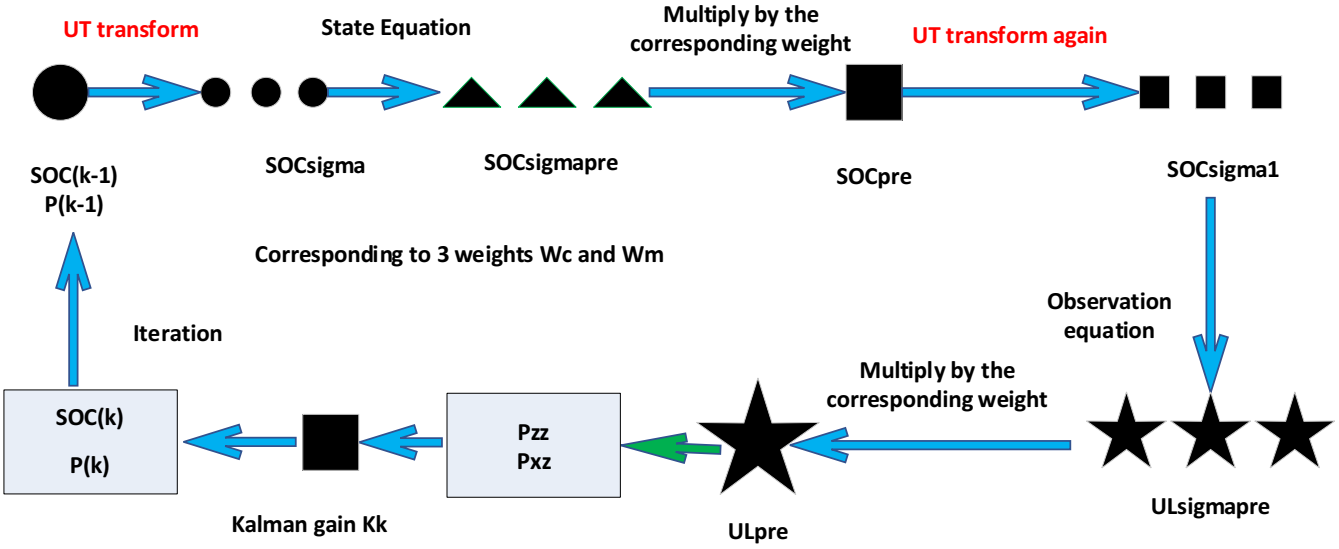

FIGURE 2 The iterate calculation process

dynamic power application conditions. The influence law of the key parameters can be revealed in the SoC estimation process. The state equation and the construction mechanism of the observation equation are explored. The random vector is calculated by using the UT nonlinear transfer probability dynamics, and the Gaussian distribution is approximated by a fixed number of sampling data points. The construction mechanism of the estimated model framework is obtained. According to the multiple input and high-non-linearity characteristics, the construction method of the equivalent model is explored combined with the operating analysis of the battery pack of the dynamic packing application conditions. Furthermore, the UT technique is used in the state equation to obtain the nonlinear transfer function of the mean and covariance. The overall implementation idea and structure block diagram are shown in Figure 2.

The theory of estimating model framework is studied by using the mathematical description of the battery characteristics in different working conditions. The equivalent model and its state-space equation can be obtained to realize the initial construction of the adaptive SoC estimation model. Furthermore, the battery equivalent model and its state-space representation are introduced into the state equation and the observation equation of the SoC estimation model. Through the tracking analysis and optimization of the SoC estimation effect, the iterate calculation process has high adaptability in describing the working state of the LIB pack. The model output response variation is studied under different conditions. The influence of current fluctuation and temperature change on the estimation accuracy is discussed. The estimation structure is optimized for the solution to the highly nonlinear problem of the LIB packs. Considering the noise optimization characterization, the basic structure of the discrete nonlinear dynamic system model can be constructed, according to which the state and measurement equations can be obtained for obtaining additional noise as shown in Equation(7).

$$\begin{cases} x_k = f\left(x_{k-1}, u_k\right) + w_k \\ y_k = g\left(x_{k-1}\right) + v_k, \end{cases} \tag{7}$$

wherein, k is the time moment. $f(\cdot)$ is the nonlinear system state transition equation. $g(\cdot)$ is the nonlinear measurement equation. $x(k)$ is the state variable. $u(k)$ is the previous known external input. $y(k)$ is the measurement signal. $w(k)$ and $v(k)$ are process and measurement noises, respectively, which are Gaussian white noises. The covariance matrix is a semipositive definite matrix. The initialization calculation can be performed as shown in Equation(8).

$$\begin{cases} t = 0, \hat{x}_0^+ = E(X_0^x), \hat{R}_{1,0}^+ = E(R_{1,0}) \\ P_{x_0}^+ = \sum_{i=0}^{2n} \omega_i^{(c)} \left(X_{0,i}^x - \hat{x}_0^+\right)\left(X_{0,i}^x - \hat{x}_0^+\right)^T \\ P_{R_{1,0}}^+ = E\left[\left(R_{1,0} - \hat{R}_{1,0}^+\right)\left(R_{1,0} - \hat{R}_{1,0}^+\right)^T\right]. \end{cases} \tag{8}$$

The weighted data points are designed to approximate the n-dimensional target sampling points, and these weighting points are calculated as well. Through the propagation of the nonlinear function, the updated filtering values are obtained through the nonlinear state equation, thereby realizing the CCV tracking target. The Sigma point sets can be obtained according to the calculation rules by the mean and variance of the state variables. These points are transferred according to the state-space model to obtain a new Sigma data point set. The weighted operation of the new point set is then used to obtain the optimal estimation of the state variables. The previous operation should be iterated repeatedly. The time update of the iterative operation is described as shown in Equation(9).

$$\begin{cases} \hat{R}_{1,t}^{-}=\hat{R}_{1,t-1}^{+} \\ P_{R_{1,t}}^{-}=P_{R_{1,t-1}}^{+}+\sigma_r \\ \hat{x}_{t/t-1}=E\left\{[F(X_{t-1,i}^{x},u_{t-1})]|_{i=0,\ldots,2n}\right\}=\sum_{i=0}^{2n}\omega_i^{m}X_{t/t-1,i}^{x} \\ \hat{y}_t=E\left\{[H(X_{t-1,i}^{x},u_t)]|_{i=0,\ldots,2n}\right\}=\sum_{i=0}^{2n}\omega_i^{(m)}y_{t/t-1,i}. \end{cases} \quad (9)$$

Combining the Sage-Husa filtering algorithm [58-60] with the UKF approach, the adaptive filtering method is introduced to correct the process noise variance, in which the measured noise variance in the formula real timely and the improved time-varying noise characteristics are applied to suit the nonlinearity. The adaptive filter can be used to obtain the measurement and updated data onto the iterative algorithm as shown in Equation(10).

$$\begin{cases} P_{x,t/t-1}=E\left[\left(x_t-\hat{x}_{t/t-1}\right)\left(x_t-\hat{x}_{t/t-1}\right)^{T}\right]=\sum_{i=0}^{2n}\omega_i^{(c)}\cdot \\ \left(X_{t/t-1,i}^{x}-\hat{x}_{t/t-1}\right)\left(X_{t/t-1,i}^{x}-\hat{x}_{t/t-1}\right)^{T}+Q \\ P_{xy,t}=\sum_{i=0}^{2n}\omega_i^{(c)}\left[X_{t/t-1,i}^{x}-\hat{x}_{t/t-1}\right]\left[y_{t/t-1,i}-\hat{y}_t\right]^{T} \\ P_{yy,t}=\sum_{i=0}^{2n}\omega_i^{(c)}\left[y_{t/t-1,i}-\hat{y}_t\right]\left[y_{t/t-1,i}-\hat{y}_t\right]^{T}+R \\ K_t=P_{xy,t}P_{yy,t}^{-1} \\ L_t^{R_1}=P_{R_{1,t}}^{-}C_t^{R_1}\left[C_t^{R_1}P_{R_{1,t}}^{-}\left(C_t^{R_1}\right)^{T}+\sigma_g\right]^{-1}. \end{cases} \quad (10)$$

Combining the battery state and internal resistance estimation methods, the improved adaptive real-time correction is investigated in the iterate calculation process. On this basis, the particle processing is simplified, and the method of estimating the battery state by RP-AUKF is obtained and realized. In the form of loop iteration, the system parameters are estimated in real time, and the estimated state is used to identify the model parameters. The SoC estimation model has good adaptive characteristics, in which the state variables and variances are estimated as shown in Equation(11).

$$\begin{cases} \hat{x}_t=\hat{x}_{t/t-1}+K_t(y_t-\hat{y}_t) \\ P_{x,t}=P_{x,t/t-1} \\ R_{1,t}^{+}=R_{1,t}^{-}+L_t^{R_1}(y_t-\hat{y}_t) \\ P_{R_{1,t}}^{+}=(I-L_t^{R_1}C_t^{R_1})P_{R_{1,t}}^{-}. \end{cases} \quad (11)$$

The system variance R can be updated according to the Equation (11), and the parameter of Q can also be updated similarly, which are used in the iterate calculation process. By designing the RP-AUKF loop iterative algorithm and constructing the model, the ohmic internal resistance is estimated in real time for the battery model, thereby improving the battery SoC estimation accuracy. Compared with the general UKF, this method improves the SoC estimation accuracy and can estimate the internal resistance value of the LIB pack accurately.

2.4 | Balance state correction

In order to solve the problem of balance state evaluation and packing SoC estimation, the numerical description and evaluation are conducted, according to which the accuracy of SoC estimation method is improved by combining the modified calculation process design. Through the comparative analysis of the advantages and disadvantages among the evaluation methods such as variance and coefficient of variation, the realization method of the balance state is evaluated by using the squared coefficient variation parameter ε, the calculation process of which is shown in Equation (12).

$$\mathrm{SoB}=\varepsilon=\theta^2=\frac{1}{n}\sum_{i=1}^{n}\left(\frac{U_{ci}-E(U_c)}{E(U_c)}\right)^2, \quad (12)$$

wherein, the abbreviation *SoB* is the shortage of state of balance, which is used to describe the voltage inconsistency degree between the internal battery cells of the LIB pack and characterized by the symbol ε. θ is used to describe the coefficient of variation between the cell battery voltages, and U_{ci} is the voltage value of the i-th battery cell obtained by measurement, and n is the number of serial connected battery cells in the LIB pack. According to the constructed adaptive SoC estimation model, the theoretical and experimental analysis is carried out to explore the balance state influence mechanism on equivalent modeling under dynamic packing application conditions. The interaction law between the cells under the packing work is analyzed, and the correction process of the equivalent model is improved. Aiming at the correction target of the equivalent modeling under the influence of balance state in the equivalent model, the voltage and internal resistance change under the influence of balance state ε which are used to characterize the consistency difference between the battery cells. The calculated expression of which is shown in Equation (13).

$$\begin{cases} U_\delta(k)=\varepsilon * U_{\mathrm{OC}}(k)=\frac{1}{n}\sum_{i=1}^{n}\left(\frac{U_{ci}(k)-E(U_c(k))}{E(U_c(k))}\right)^2 * U_{\mathrm{OC}}(k) \\ R_\delta(k)=\varepsilon * R_o(k)=\frac{1}{n}\sum_{i=1}^{n}\left(\frac{U_{ci}(k)-E(U_c(k))}{E(U_c(k))}\right)^2 * R_o(k). \end{cases} \quad (13)$$

On the basis of simulation and experimental analysis, the balance state is mathematically described. The influence of balance state is incorporated into the iterative calculation process, and then, the model parameters and weighting factors are modified, according to which the proposed equivalent model is improved. The intermittent aging degree measurement and

real-time calibration calculation process are combined with the parameter identification and iterate calculation algorithm. Through the research on the equivalent modeling method of the dynamic application environment, the structural model is constructed for the SoC estimation combined with the parameter identification. By carrying out the standard 1C discharge capacity measurement experiment, the actual electric quantity $Q_{\text{n\_Deter}}$ is obtained by using the Ah integration method. This parameter is characterized by the SoC at the end time point of the discharge, which is described by using the symbol S_{n}. The rated capacity $Q_{\text{n\_Rated}}$ provided by the battery manufacturer is characterized by SoC_0. Furthermore, the relative variation ratio of SoC named as δ_{S} can be obtained. The calculation process is shown in Equation (14).

$$\begin{cases} K_{\text{Q}} = \delta_{\text{S}} = \dfrac{S_n}{S_0} \times 100\% = \dfrac{Q_{n\_\text{Deter}}}{Q_{0\_\text{Rated}}} \times 100\% \\ Q_n = K_{\text{Q}} Q_{n\_\text{Rated}} - \Delta Q_n, \Delta Q_n = f(N). \end{cases} \tag{14}$$

In the formula, N is the number of charge-discharge cycles after the most recent capacity measurement, and ΔQ_{n} is the influence of the subsequent cycle number on the rated capacity. Furthermore, the aging characteristic influence on the rated capacity is considered for the correction treatment of the equivalent modeling process. The initial SoC value is maintained after the full charge maintenance by conducting the equalization charging method, and the SoC variation is the normalized representation of Q_{n}. The influence coefficient K_{Q} of the aging state can be obtained on the electric quantity Q_{n}. Since the aging process is a slowly changing process, the functional relationship is determined by periodically measuring the calibration. The functional relationship can be obtained by the synchronous acquisition and correction of the correlation between the rated capacity and the charge-discharge cycling number. By superimposing the effects of the two parts, the corrected capacity value of the aging factor can be obtained.

3 | EXPERIMENTAL ANALYSIS

The embedded verification of the proposed equivalent modeling method is realized by the development of the BMS. Considering the different initial power conditions and equivalent model parameters, the experimental analysis of the initial condition influence is carried out on the estimation accuracy. The experimental analysis under variable multirate current conditions is carried out to study the dynamic relationship between the working condition change and the equivalent modeling results. The experimental analysis of the phased simulation is carried out by the short-time discharge, different time-length combination, and long-time discharge experiments. Furthermore, the estimation and correction effects are carried out for the complex working conditions and the reliable verification is finally realized.

3.1 | Characteristic experiments

The test battery is the ternary LIB with a rated capacity of 50 Ah, and the battery charging and discharging equipment is provided by Shenzhen Yakeyuan Technology Co., Ltd., the name of which is BTS200-100-104 battery testing equipment. The overall implemented system is shown in Figure 3.

The experiment uses the equivalent model to observe the influence of its related parameters on SoC and the relationship between OCV and SoC is shown in Figure 4.

The standard HPPC test is carried out for LIBs at 10 SoC points of 0.1, 0.2, …, 0.9, 1.0, respectively, and the charge-discharge current is set to be 50A (1C). The sequence of the single cycle contains 10s constant current discharge pulses, 40s hold, and 10s constant current charge pulses. And the 10 SoC pulse cycles are separated by 1 hour. The corresponding voltage varying curve along with the current pulse changes in the HPPC test is shown in Figure 5.

As can be seen from the battery voltage response curve in the HPPC test, the model parameters of the 10 SoC points can be extracted and characterized as follows. (1) The voltage at the discharge start time t_1 and the discharge stopped time t_2 will be changed vertically, which is a voltage transient due to the presence of the battery ohmic internal resistance. (2) The battery terminal voltage drops slowly during the time period of t_1-t_2 which can be characterized by the charging process of the polarization capacitor to the polarization current, producing a zero-state response to the dual RC series circuit. (3) During the period from t_2 to t_3, the battery terminal voltage rises slowly, which is the discharging process from the polarization capacitance to the polarization resistance, expressing the zero input response to the dual RC series circuit. (4) The battery terminal voltage U_1 before the discharge pulse is slightly higher than the terminal voltage U_5 at the end of the discharge and reaching the steady state, which is the voltage difference caused by the integration of the discharge current on the storage capacitor. The ohmic values in the improved model can be obtained directly by feature 1 and 4. The polarization resistance and polarization capacitance values in the dual RC circuit can be obtained by the cells of feature 2 and 3, according to which the end voltage curve is identified.

3.2 | Parameter identification

The parameter in the proposed ECM not only changes along with the SoC level but also varying along with the aging process, so that the cycling HPPC tests are investigated in the long-time cycling process, which will be expressed in the full life cycling SoC estimation of the power LIBs. According to the above test procedure, the terminal voltage output waveform in the HPPC test can be obtained as shown in Figure 6.

According to the above experimental design, the corresponding data onto the parameters at each SoC point can be obtained according to the various model parameter identification. The charge-discharge current and terminal voltage values obtained from the HPPC test are introduced into the current

FIGURE 3 The implemented system

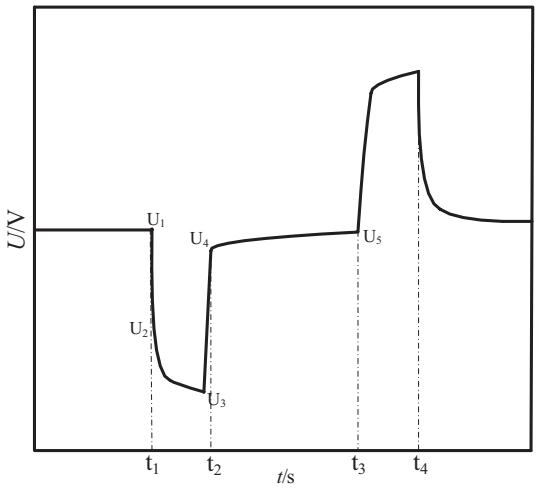

FIGURE 5 The Hybrid Pulse Power Characteristic experiment

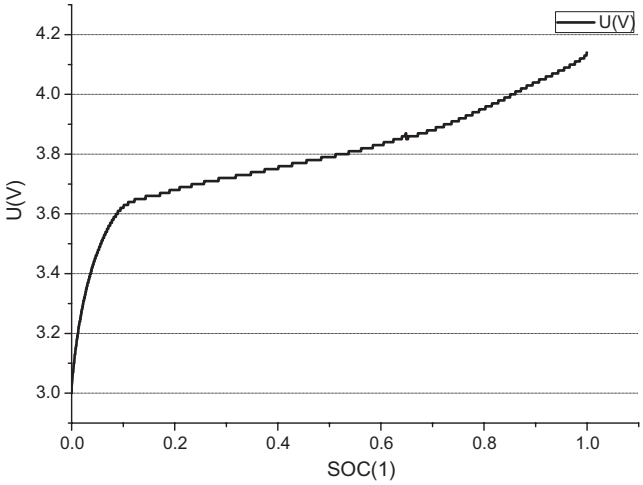

FIGURE 4 The OCV-SoC relationship

module and the voltage module, respectively, in the form of data. The R_o can be obtained by the curve fitting, respectively. R_{cd}, R_p, C_p and OCV-SoC six polynomial functions are input into the model parameter update subsystem for simulation. The parameter identification results are shown in Table 1.

3.3 | Voltage tracking results with HPPC test

The parameter values of the improved model can be obtained by the above identification, which are verified under different SoC levels. The charge-discharge current values of the HPPC test and the battery terminal voltage values are, respectively, introduced into the current module and the voltage module in the form of data. The simulated and measured terminal voltage comparison curves are obtained. The experimental results of the parameter dialectical test are shown in Figure 7.

The experimental results can be obtained from the error curve of the simulated voltage and the real-time detected voltage under the illustrated periodic current discharge. The battery terminal voltage will suddenly change along with the current pulse, resulting in an error increase between the experimental value of the lower terminal voltage and the estimated value at the same time to 0.1-0.2 V. After several times of HPPC test results with different discharge current rates, the battery terminal voltage error is large along with the current pulse due to environmental factors and measurement deviations. When the battery SoC changes into the range of 0 ~ 10%, the experimental value of the terminal voltage and the simulated value is slightly larger than the SoC value of 10%~100%. This is mainly because the battery is close to the end of discharge when the SoC is <10%. The internal electrochemical reaction changes drastically, and the values of various parameters in the battery model are changed greatly.

Except for the abovementioned individual time moments, when the SoC value changes of 10% ~ 100%, the simulated value of the terminal voltage is consistent with the experimental value. The voltage tracking error is <0.035 V, accounting for 0.9% of the nominal voltage. The above analysis fully shows that the improved model is reasonable and the parameter identification accuracy is high. The improved circuit model and the parameter identification can provide a theoretical accurate estimation basis of the internal LIB state variables.

3.4 | Estimation effect under complex conditions

The parameter values of the improved model under different SoC states can be obtained by the above identification. The experimental SoC estimation results can be obtained by using the intermittent main discharge and shelving test experiments, in which the discharging current varies greatly in the intermittent HPPC test. The estimated SoC curves can be obtained, and the results of the parameter dialectical test are shown in Figure 8.

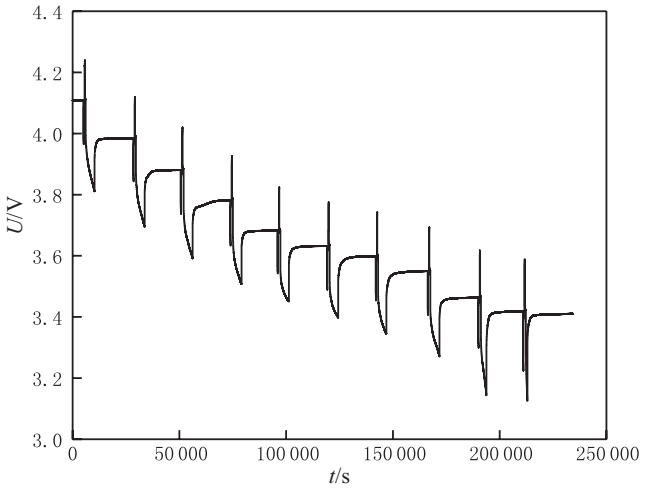

FIGURE 6 The voltage curve of Hybrid Pulse Power Characteristic test

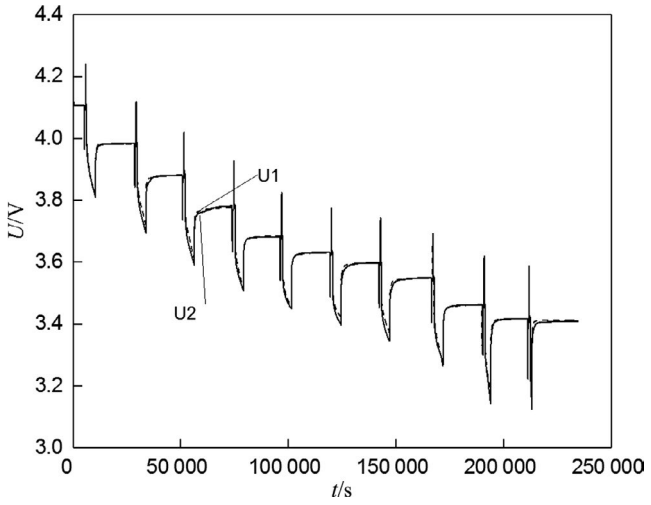

FIGURE 7 The voltage tracking result

TABLE 1 Model parameter identification result

SoC	R_o (Ω)	R_{cd} (Ω)	C_p (F)	R_p (Ω)	E (V)	τ
1	0.0016	0.000899	14505.5774	0.001300	4.17	18.85725
0.975	0.0016	0.000924	15620.1187	0.001000	4.13	15.62012
0.950	0.0016	0.000930	29025.8911	0.001100	4.10	31.92848
0.925	0.0016	0.000923	29372.8888	0.001100	4.07	32.31018
0.9	0.0016	0.000908	29372.8888	0.001100	4.04	32.31018
0.8	0.0015	0.000827	15426.6233	0.001100	3.93	16.96929
0.7	0.0014	0.000801	10027.7769	0.001300	3.83	13.03611
0.6	0.0015	0.000853	29699.1476	0.001100	3.73	32.66906
0.5	0.0015	0.000946	27510.3164	0.001000	3.66	27.51032
0.4	0.0015	0.001036	11678.3456	0.000911	3.62	10.64283
0.3	0.0014	0.001126	2613.70653	0.000953	3.58	2.491281
0.2	0.0016	0.001321	17867.3528	0.001200	3.52	21.44082
0.1	0.0019	0.001887	10006.0036	0.002000	3.43	20.01201

According to the statistical characteristics and modeling analysis under complex conditions, the influencing factors are integrated into the ECM by using the modular circuit equivalent method. When the remaining energy varies from 10% to 100%, the SoC estimation accuracy is 98.56%. A characteristic model is established that is capable of describing the life cycle behavior of the LIBs. Then, the state-space description analysis is carried out, which is constructed to express the working characteristics accurately. The mathematical description of the working characteristics can be investigated for the LIB pack of complex conditions and the CCV tracking result is shown in Figure 9.

Combined with the working characteristic analysis, the equivalent accuracy of the ECM is improved. The state-space equivalent theory is introduced, according to which the weight calculation process is improved and the aging coefficient is superimposed. Furthermore, the accurate simulation is realized for the LIB working characteristics, which solves the problem that the parameter convergence speed is slow and the estimation is inaccurate due to the coupling of the battery model parameters. The validation experiments have the same changing law with the reference,[61] which verifies that the accurate SoC estimation results can be obtained by using the proposed working state estimation of the power LIBs. Through data-driven life cycling state estimation, the key factors affecting battery aging are further revealed and the CCV tracking error is shown in Figure 10.

The experimental results can be obtained from the error curve of the simulated voltage and the real voltage under the periodic current discharge treatment. When the remaining energy varies from 10% to 100%, the tracking voltage error is <0.035 V. The battery terminal voltage will be abrupt toward the current pulse. When the battery SoC value changes into the range of 0 ~ 10%, the experimental value of the terminal voltage and the simulated value are slightly larger than the SoC value of 10%~100%. This is mainly because the LIB is close to the end of discharge when the SoC is <10%. The

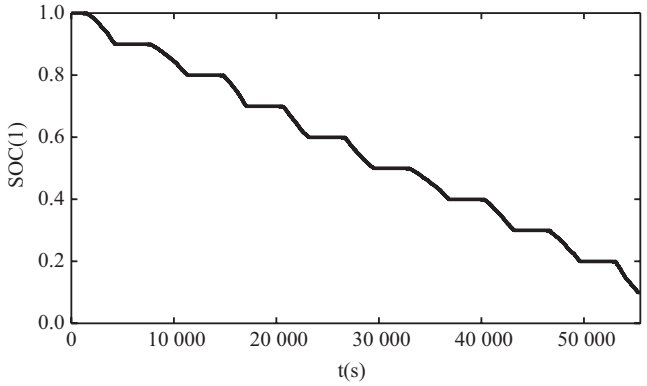

FIGURE 8 The working state estimation effects

internal electrochemical reaction changes drastically, and the values of various parameters in the battery model are greatly changed. In addition to the abovementioned individual time moments, when the SoC value changes, the simulated value of the terminal voltage is consistent with the experimental value.

3.5 | Multirate combined working condition test

Considering the complexity of the working conditions, the experiment of complex rate discharge simulation is designed according to the dynamic load profile of the Federal Urban Driving

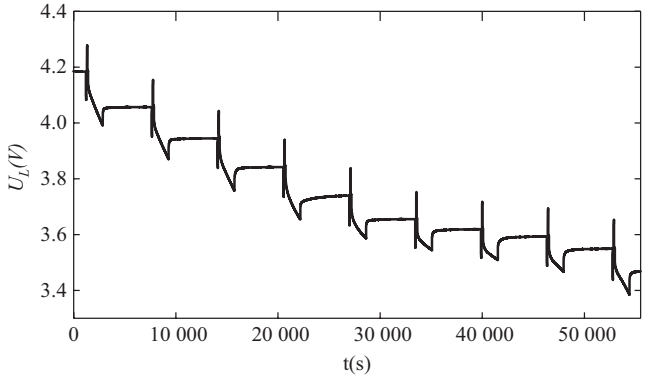

FIGURE 9 The closed circuit voltage tracking result

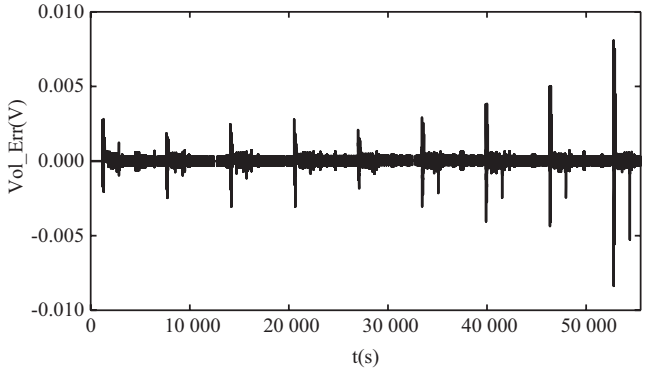

FIGURE 10 The closed circuit voltage tracking error

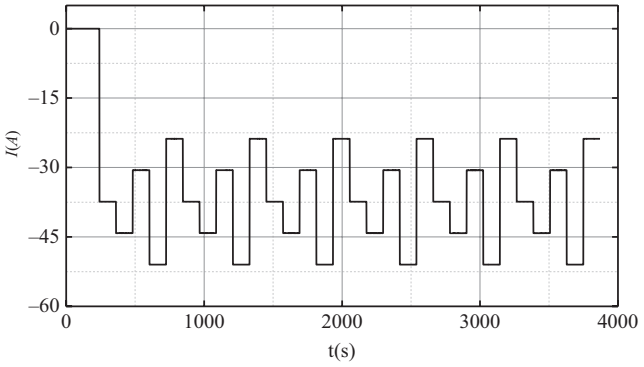

FIGURE 11 Multirate working condition current curve

Schedule (FUDS) to further verify the applicability of the proposed algorithm to complex working conditions. The current variation is designed for the complex working conditions. The pulse discharge experiments of different currents are used to analyze and describe the working characteristics of the LIB pack more accurately, and to describe its working characteristics. In the experimental process, the different discharge current magnification (0.35C, 0.45C, 0.55C, 0.65C, and 0.75C) varies depending on the current simulation experiment as shown in Figure 11.

The SoC estimation performance test is realized under complex variable current conditions, and the new model is further verified, which is convergence to complex current changes. In the experimental analysis of the complex conditions of the power LIBs, the terminal voltage and SoC values are obtained as shown in Figure 12.

The experiments of designing complex rate discharge conditions are carried out to verify further the applicability of the proposed model into complex working conditions. The results show that the model has good dynamic performance and the model accuracy is high, which can provide a theoretical basis for the accurate SoC estimation of the internal LIB state variables.

4 | CONCLUSIONS

Aiming to realize high-precision SoC estimation of the power LIB packs, a novel iterative calculation method is proposed

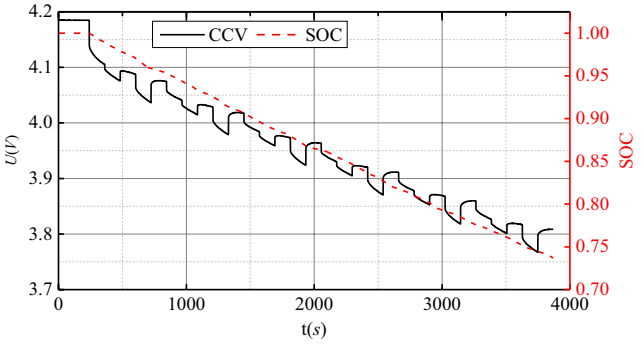

FIGURE 12 Multirate combined operating SoC curve

and the splice equivalent circuit modeling is revealed to the complex current conditions, breaking the shortcomings of traditional equivalent modeling and SoC estimation technologies. Combined with state-space equation description and balance state correction strategy research, a full life cycling SoC estimation model is established for the power LIBs, in which a novel particle adaptive unscented Kalman filtering algorithm is introduced in the iterative calculation process. The proposed SoC estimation theory has high precision and robustness advantages, which lays a key breakthrough foundation for the energy management of the power LIB packs.

ACKNOWLEDGMENTS

The work was supported by National Natural Science Foundation of China (No. 61801407). CF would like to express his gratitude to RGU for its support.

ORCID

Shun-Li Wang https://orcid.org/0000-0003-0485-8082

REFERENCES

1. Wang Z, Zeng S, Guo J, Qin T. State of health estimation of lithium-ion batteries based on the constant voltage charging curve. *Energy*. 2019;167:661-669.
2. Wang XY, Wei XZ, Dai HF. Estimation of state of health of lithium-ion batteries based on charge transfer resistance considering different temperature and state of charge. *J Energy Stor*. 2019;21:618-631.
3. Couto LD, Schorsch J, Job N, Léonard A, Kinnaert M. State of health estimation for lithium ion batteries based on an equivalent-hydraulic model: An iron phosphate application. *J Energy Stor*. 2019;21:259-271.
4. Chen Z, Sun H, Dong G, Wei J, Wu JI. Particle filter-based state-of-charge estimation and remaining-dischargeable-time prediction method for lithium-ion batteries. *J Power Sources*. 2019;414:158-166.
5. Cai L, Meng J, Stroe D-I, Luo G, Teodorescu R. An evolutionary framework for lithium-ion battery state of health estimation. *J Power Sources*. 2019;412:615-622.
6. Zheng Y, Ouyang M, Han X, Lu L, Li J. Investigating the error sources of the online state of charge estimation methods for lithium-ion batteries in electric vehicles. *J Power Sources*. 2018;377:161-188.
7. Zheng Y, Gao W, Ouyang M, Lu L, Zhou L, Han X. State-of-charge inconsistency estimation of lithium-ion battery pack using mean-difference model and extended Kalman filter. *J Power Sources*. 2018;383:50-58.
8. Zheng L, Zhu J, Wang G, Lu D-C, He T. Differential voltage analysis based state of charge estimation methods for lithium-ion batteries using extended Kalman filter and particle filter. *Energy*. 2018;158:1028-1037.
9. Wang Y, Liu C, Pan R, Chen Z. Modeling and state-of-charge prediction of lithium-ion battery and ultracapacitor hybrids with a co-estimator. *Energy*. 2017;121:739-750.
10. Zheng L, Zhu J, Lu D-C, Wang G, He T. Incremental capacity analysis and differential voltage analysis based state of charge and capacity estimation for lithium-ion batteries. *Energy*. 2018;150:759-769.
11. Zhao WZ, Kong XC, Wang CY. Combined estimation of the state of charge of a lithium battery based on a back-propagation-adaptive Kalman filter algorithm. *Proc Inst Mech Eng D J Automob Eng*. 2018;232(3):357-366.
12. Zhang XU, Wang Y, Wu JI, Chen Z. A novel method for lithium-ion battery state of energy and state of power estimation based on multi-time-scale filter. *Appl Energy*. 2018;216:442-451.
13. Zhang W, Wang L, Wang L, Liao C. An improved adaptive estimator for state-of-charge estimation of lithium-ion batteries. *J Power Sources*. 2018;402:422-433.
14. Zhang R, Xia B, Li B, Cao L, Lai Y, Zheng W, et al. State of the art of lithium-ion battery SOC estimation for electrical vehicles. *Energies*. 2018;11(7): 1820.
15. Zeng ZB, Tian J, Li D, Tian Y. An online state of charge estimation algorithm for lithium-ion batteries using an improved adaptive cubature Kalman filter. *Energies*. 2018;11(1):59.
16. Wang Q-K, He Y-J, Shen J-N, Hu X-S, Ma Z-F. State of charge-dependent polynomial equivalent circuit modeling for electrochemical impedance spectroscopy of lithium-ion batteries. *IEEE Trans Power Electron.*. 2018;33(10):8449-8460.
17. Ye M, Guo H, Xiong R, Yu Q. A double-scale and adaptive particle filter-based online parameter and state of charge estimation method for lithium-ion batteries. *Energy*. 2018;144:789-799.
18. Yang J, Xia B, Huang W, Fu Y, Mi C. Online state-of-health estimation for lithium-ion batteries using constant-voltage charging current analysis. *Appl Energy*. 2018;212:1589-1600.
19. Yang D, Wang Y, Pan R, Chen R, Chen Z. State-of-health estimation for the lithium-ion battery based on support vector regression. *Appl Energy*. 2018;227:273-283.
20. Xie JL, Ma JC, Bai K. Enhanced coulomb counting method for state-of-charge estimation of lithium-ion batteries based on Peukert's law and coulombic efficiency. *J Power Electron*. 2018;18(3):910-922.
21. Xiang S, Hu G, Huang R, Guo F, Zhou P. Lithium-Ion battery online rapid state-of-power estimation under multiple constraints. *Energies*. 2018;11(2): 283.
22. Xia B, Zhang Z, Lao Z, Wang W, Sun W, Lai Y, et al. Strong tracking of a H-infinity filter in lithium-ion battery state of charge estimation. *Energies*. 2018;11(6): 1481.
23. Liu XY, Li WL, Zhou AG. PNGV equivalent circuit model and SOC estimation algorithm for lithium battery pack adopted in AGV vehicle. *IEEE Access*. 2018;6:23639-23647.
24. Xia B, Guo S, Wang W, et al. A state of charge estimation method based on adaptive extended Kalman-Particle filtering for lithium-ion batteries. *Energies*. 2018;11(10): 2755.
25. Xia B, Cui D, Sun Z,et al. State of charge estimation of lithium-ion batteries using optimized Levenberg-Marquardt wavelet neural network. *Energy*. 2018;153:694-705.
26. Wu XG, Li XF, Du JY. State of charge estimation of lithium-ion batteries over wide temperature range using unscented Kalman filter. *IEEE Access*. 2018;6:41993-42003.
27. Wei Z, Zhao J, Zou C, Lim TM, Tseng KJ. Comparative study of methods for integrated model identification and state of charge estimation of lithium-ion battery. *J Power Sources*. 2018;402:189-197.
28. Wei Z, Leng F, He Z, Zhang W, Li K. Online state of charge and state of health estimation for a lithium-ion battery based on a data-model fusion method. *Energies*. 2018;11(7): 1810.

29. Zou CF, Hu X, Dey S, Zhang L, Tang X. Nonlinear fractional-order estimator with guaranteed robustness and stability for lithium-ion batteries. *IEEE Trans Industr Electron*. 2018;65(7):5951-5961.
30. Wang X, Xu J, Zhao YF. Wavelet based denoising for the estimation of the state of charge for lithium-ion batteries. *Energies*. 2018;11(5): 1144.
31. Wang T, Chen S, Ren H, Zhao Y. Model-based unscented Kalman filter observer design for lithium-ion battery state of charge estimation. *Int J Energy Res.*. 2018;42(4):1603-1614.
32. Wang SL, Yu C-M, Fernandez C, Chen M-J, Li G-L, Liu XH. Adaptive state-of-charge estimation method for an aeronautical lithium-ion battery pack based on a reduced particle-unscented Kalman filter. *J Power Electron*. 2018;18(4):1127-1139.
33. Wang S, Fernandez C, Shang L, Li Z, Yuan H. An integrated online adaptive state of charge estimation approach of high-power lithium-ion battery packs. *Trans Inst Meas Control*. 2018;40(6):1892-1910.
34. Tsai I-H, Yu K-H, Tseng A, Yen J-Y, Fu T-T, Huang E. Battery cell modeling and online estimation of the state of charge of a lithium-ion battery. *J Chin Inst Eng*. 2018;41(5):412-418.
35. Tran N-T, Khan A, Nguyen T-T, Kim D-W, Choi W. SOC estimation of multiple lithium-ion battery cells in a module using a nonlinear state observer and online parameter estimation. *Energies*. 2018;11(7): 1620.
36. Tang X, Zou C, Yao KE, Chen G, Liu B, He Z, et al. A fast estimation algorithm for lithium-ion battery state of health. *J Power Sources*. 2018;396:453-458.
37. Stroe A-I, Meng J, Stroe D-I, Świerczyński M, Teodorescu R, Kær S. Influence of battery parametric uncertainties on the state-of-charge estimation of lithium titanate oxide-based batteries. *Energies*. 2018;11(4): 795.
38. Shen P, Ouyang M, Lu L, Li J, Feng X. The co-estimation of state of charge, state of health, and state of function for lithium-ion batteries in electric vehicles. *IEEE Trans Veh Technol*. 2018;67(1):92-103.
39. Salameh M, Wilke S, Schweitzer B, Sveum P, Al-Hallaj S, Krishnamurthy M. Thermal state of charge estimation in phase change composites for passively cooled lithium-ion battery packs. *IEEE Trans. Ind. Appl.*. 2018;54(1):426-436.
40. Peng S, Zhu X, Xing Y, Shi H, Cai XU, Pecht M. An adaptive state of charge estimation approach for lithium-ion series-connected battery system. *J Power Sources*. 2018;392:48-59.
41. Park J, Lee B, Jung DY, Kim DH. Battery state estimation algorithm for high-capacity lithium secondary battery for EVs considering temperature change characteristics. *J Elec Eng Technol*. 2018;13(5):1927-1934.
42. Ning BO, Cao B, Wang B, Zou Z. Adaptive sliding mode observers for lithium-ion battery state estimation based on parameters identified online. *Energy*. 2018;153:732-742.
43. Meng J, Luo G, Ricco M, Swierczynski M, Stroe D-I, Teodorescu R. Overview of lithium-ion battery modeling methods for state-of-charge estimation in electrical vehicles. *Appl Sci Basel*. 2018;8(5): 659.
44. Meng J, Cai L, Luo G, Stroe D-I, Teodorescu R. Lithium-ion battery state of health estimation with short-term current pulse test and support vector machine. *Microelectron Reliab*. 2018;88-90:1216-1220.
45. Lu X, Li H, Xu J, Chen S, Chen N. Rapid estimation method for state of charge of lithium-ion battery based on fractional continual variable order model. *Energies*. 2018;11(4): 714.
46. Lu J, Chen Z, Yang Y, Lv M. Online estimation of state of power for lithium-ion batteries in electric vehicles using genetic algorithm. *IEEE Access*. 2018;6:20868-20880.
47. Tang X, Gao F, Zou C, Yao KE, Hu W, Wik T. Load-responsive model switching estimation for state of charge of lithium-ion batteries. *Appl Energy*. 2019;238:423-434.
48. Liu Z, Dang XJ. A new method for state of charge and capacity estimation of lithium-ion battery based on dual strong tracking adaptive H infinity filter. *Math Probl Eng*. 2018.
49. Liu D, Yin X, Song Y, Liu W, Peng YU. An on-line state of health estimation of lithium-ion battery using unscented particle filter. *IEEE Access*. 2018;6:40990-41001.
50. Lipu M, Hannan MA, Hussain A, Saad M, Ayob A, Blaabjerg F. State of charge estimation for lithium-ion battery using recurrent NARX neural network model based lighting search algorithm. *IEEE Access*. 2018;6:28150-28161.
51. Lipu M, Hannan MA, Hussain A, et al. A review of state of health and remaining useful life estimation methods for lithium-ion battery in electric vehicles: Challenges and recommendations. *J Clean Prod*. 2018;205:115-133.
52. Li J, Adewuyi K, Lotfi N, Landers RG, Park J. A single particle model with chemical/mechanical degradation physics for lithium ion battery State of Health (SOH) estimation. *Appl Energy*. 2018;212:1178-1190.
53. Li GD, Peng K, Li B. State-of-charge estimation for lithium-ion battery using a combined method. *J Power Electron*. 2018;18(1):129-136.
54. Zou C, Manzie C, Nešić D, Kallapur AG. Multi-time-scale observer design for state-of-charge and state-of-health of a lithium-ion battery. *J Power Sources*. 2016;335:121-130.
55. Li B, Peng K, Li GD. State-of-charge estimation for lithium-ion battery using the Gauss-Hermite particle filter technique. *J Renew Sust Energy*. 2018;10(1): 014105.
56. Lee KT, Dai MJ, Chuang CC. Temperature-compensated model for lithium-ion polymer batteries with extended Kalman filter state-of-charge Estimation for an Implantable Charger. *IEEE Trans Industr Electron*. 2018;65(1):589-596.
57. Wang YJ, Zhang CB, Chen ZH. A method for joint estimation of state-of-charge and available energy of LiFePO4 batteries. *Appl Energy*. 2014;135:81-87.
58. Sun J, Xu X, Liu Y, Zhang T, Li Y. FOG random drift signal denoising based on the improved ar model and modified Sage-Husa adaptive Kalman filter. *Sensors*. 2016;16(7):1073.
59. Gao K, Ren S, Yi G, Zhong J, Wang Z. An improved ACKF/kf initial alignment method for odometer-aided strapdown inertial navigation system. *Sensors*. 2018;18(11):3896.
60. Peng S, Chen C, Shi H, Yao Z. State of charge estimation of battery energy storage systems based on adaptive unscented Kalman Filter with a noise statistics estimator. *IEEE Access*. 2017;5:13202-13212.
61. Wang YJ, Zhang CB, Chen ZH. A method for state-of-charge estimation of LiFePO4 batteries at dynamic currents and temperatures using particle filter. *J Power Sources*. 2015;279:306-311.

How to cite this article: Cao W, Wang S-L, Fernandez C, Zou C-Y, Yu C-M, Li X-X. A novel adaptive state of charge estimation method of full life cycling lithium-ion batteries based on the multiple parameter optimization. *Energy Sci Eng*. 2019;00:1–13. https://doi.org/10.1002/ese3.362